arXiv:hep-ph/0208163v2 20 Aug 2002

Fermilab-Pub-02/184-T
IFT-P.052/2002
hep-ph/0208163
August 15, 2002

Parameter Degeneracies in Neutrino Oscillation Measurement of Leptonic CP and T Violation

Hisakazu Minakata[1], Hiroshi Nunokawa[2], Stephen Parke[3]

[1] *Department of Physics, Tokyo Metropolitan University*
1-1 Minami-Osawa, Hachioji, Tokyo 192-0397, Japan
minakata@phys.metro-u.ac.jp

[2] *Instituto de Física Teórica, Universidade Estadual Paulista*
Rua Pamplona 145, 01405-900 São Paulo, SP Brazil
nunokawa@ift.unesp.br

[3] *Theoretical Physics Department, Fermi National Accelerator Laboratory*
P.O.Box 500, Batavia, IL 60510, USA
parke@fnal.gov

Abstract

The measurement of the mixing angle θ_{13}, sign of Δm^2_{13} and the CP or T violating phase δ is fraught with ambiguities in neutrino oscillation. In this paper we give an analytic treatment of the paramater degeneracies associated with measuring the $\nu_\mu \to \nu_e$ probability and its CP and/or T conjugates. For CP violation, we give explicit solutions to allow us to obtain the regions where there exist two-fold and four-fold degeneracies. We calculate the fractional differences, $(\Delta\theta/\bar{\theta})$, between the allowed solutions which may be used to compare with the expected sensitivities of the experiments. For T violation we show that there is always a complete degeneracy between solutions with positive and negative Δm^2_{13} which arises due to a symmetry and cannot be removed by observing one neutrino oscillation probability and its T conjugate.

Thus, there is always a four fold parameter degeneracy apart from exceptional points. Explicit solutions are also given and the fractional differences are computed. The bi-probability CP/T trajectory diagrams are extensively used to illuminate the nature of the degeneracies.

Typeset using REVTEX

I. INTRODUCTION

The discovery of neutrino oscillation in atmospheric neutrino observation in Super-Kamiokande [1] and the recent accumulating evidences for solar neutrino oscillations [2] naturally suggests neutrino masses and lepton flavor mixing. It is also consistent with the result of the first man-made beam long-baseline accelerator experiment K2K [3]. Given the new realm of lepton flavor mixing whose door is just opened, it is natural to seek for a program of exploring systematically the whole structure of neutrino masses and lepton flavor mixing.

Most probably, the most difficult task in determining the structure of lepton mixing matrix, the Maki-Nakagawa-Sakata (MNS) matrix [4], is determination of CP violating phase δ and a simultaneous (or preceding) measurement of $|U_{e3}| = \sin\theta_{13}$. We use in this paper the standard notation for the MNS matrix with $\Delta m^2_{ij} \equiv m^2_j - m^2_i$. The fact that the most recent analyses of the solar neutrino data [5] strongly favor the large mixing angle (LMA) Mikheev-Smirnov-Wolfenstein (MSW) solution [6] is certainly encouraging for any attempts to measure leptonic CP violation.

Since we know that θ_{13} is small, $\sin^2 2\theta_{13} \lesssim 0.1$, due to the constraint imposed by the Chooz reactor experiment [7] and we do not know how small it is, there is two different possibilities. Namely, (A) θ_{13} is determined prior to the experimental search for leptonic CP violation, or (B) not. The case (A) is desirable experimentally. To determine unknown quantities one by one, if possible, is the most sensible way to proceed with minimal danger of picking up fake effects. But since there is no guarantee that the case (A) *is* the case, we must prepare for the case (B). Even in the case (A), experimental determination of θ_{13} always comes with errors, and one must face with the similar problem as in the case B within the experimental uncertainties. Moreover, it is known that determination of θ_{13} in low energy conventional super-beam type experiments suffers from additional intrinsic uncertainty, the one coming from unknown CP violating phase δ. See Ref. [8] for further explanation and a possible way of circumventing the problem. Therefore, the determination of δ and θ_{13} are

inherently coupled with one another.

Even more seriously, it was noticed by Burguet-Castell *et al.* [9] that there exist two sets of degenerate solutions $(\delta_i, \theta_{13}^i)$ (i=1, 2) even if oscillation probabilities of $P(\nu_\mu \to \nu_e) \equiv P(\nu)$ and its CP conjugate, $\mathrm{CP}[P(\nu)] \equiv P(\bar{\nu}_\mu \to \bar{\nu}_e)$ is accurately measured. They presented an approximate but transparent framework of analyzing the degeneracy problem, which we follow in this paper. It was then recognized in Ref. [10] that unknown sign of Δm^2_{13} leads to a duplication of the ambiguity, which entails maximal four-fold degeneracy (see below). It was noticed by Barger *et al.* [11] that the four-fold degeneracy is further multiplied by an ambiguity due to approximate invariance of the oscillation probability under the transformation $\theta_{23} \to \frac{\pi}{2} - \theta_{23}$. A special feature of the degeneracy problem at the oscillation maximum was noted and analyzed to some detail [8,11]. Recently, the first discussion of the problem of parameter degeneracy in T violation measurement is given in Ref. [12].

Meanwhile, there were some technological progresses in analyzing the interplay between the genuine CP phase and the matter effects in measuring leptonic CP or T violation in neutrino oscillation, the issue much-discussed but still unsettled [13,14]. The authors of Refs. [10] and [12] introduced, respectively, the "CP and T trajectory diagrams in bi-probability space" for pictorial representation of CP-violating and CP-conserving phase effects as well as the matter effect in neutrino oscillations. They showed that when these two types of trajectory diagrams are combined it gives a unified graphical representation of neutrino oscillations in matter [12]. We demonstrate in this paper that they provide a powerful tool for understanding and analyzing the problem of parameter degeneracy, as partly exhibited in Refs. [10,15,11].

It is the purpose of this paper to give a completely general treatment of the problem of parameter degeneracy in neutrino oscillations associated with CP and T violation measurements. We elucidate the nature of the degeneracy, and determine the region where it occurs, namely, the regions in the P-CP[P] (and P-T[P]) bi-probability space in which the same-Δm^2_{13}-sign and/or the mixed-Δm^2_{13}-sign degeneracies take place. While partial treatment

of the parameter degeneracy has been attempted for CP measurement before [8–11] such general treatment is still lacking. We believe that it is worthwhile to have such an overview of the parameter degeneracy issue to uncover ways of resolving this problem. See [16–19] for recent discussions.

We present the first systematic discussion of parameter degeneracy in T measurement following our previous paper in which we set up the problem [12]. We uncover a new feature of the degeneracy in T measurement. Namely, we show that for a given T trajectory diagram there always exists an another T diagram which completely degenerates with the original one and has opposite sign of Δm^2_{13}. It means that for any given values of $P(\nu)$ and T$[P(\nu)]$ there is two degenerate solutions of $(\delta,\, \theta_{13})$ with differing sign of Δm^2_{13}. It should be noticed that this is true no matter how large the matter effect, quite contrary to the case of CP measurement. Therefore, determination of the signs of Δm^2_{13} is impossible in a single T measurement experiment unless one of the following conditions is met; (a) one of the solutions is excluded, for example, by the CHOOZ constraint, or (b) some additional information, such as energy distribution of the appearance electrons, is added.

We emphasize that a complete understanding of the structure of the parameter degeneracy should be helpful for one who want to pursue solution of the ambiguity problem in an experimentally realistic setting. We, however, do not attempt to discuss the $\theta_{23} \leftrightarrow \frac{\pi}{2} - \theta_{23}$ degeneracy. We also do not try to solve the problem of parameter degeneracy exactly though it is in principle possible by using an exact but reasonably compact expression of the oscillation probability obtained by Kimura, Takamura, and Yokomakura [20]. Instead, we restrict ourselves into the treatment with the approximation introduced by Burguet-Castell *et al.* [9] in which the approximate formula for the oscillation probability derived by Cervera *et al.* [21] was employed. Though not exact, it gives us much more transparent overview of the problem of parameter degeneracy.

II. PROBLEM OF PARAMETER AMBIGUITY IN CP AND T VIOLATION MEASUREMENT

We define the "CP (T) parameter ambiguity" as the problem of having multiple solutions of (δ, θ_{13}) and the sign of Δm^2_{23}, for a given set of measured values of oscillation probabilities of $P(\nu_\mu \to \nu_e)$ and its CP (T) conjugate, $\mathrm{CP}[P(\nu)] \equiv P(\bar{\nu}_\mu \to \bar{\nu}_e)$ ($\mathrm{T}[P(\nu)] \equiv P(\nu_e \to \nu_\mu)$). We concentrate in this paper on this channel because precise measurement is much harder in other channels, e.g., in $\nu_e \to \nu_\tau$. Our use of $\nu_\mu \to \nu_e$ and its CP-conjugate is due to our primary concern on conventional super-beam type experiments [22]. The reader should keep this difference in mind if they try to compare our equations with those in Refs. [9,12] in which they use $\nu_e \to \nu_\mu$ and its CP-conjugate, a natural choice for neutrino factories [21,23]. It should also be noted that the neutrino factories and the superbeam experiments are studying processes which are T-conjugates.

In this section we utilize the CP and the T trajectory diagrams introduced in [10] and [12], respectively, to explain what is the problem of parameter ambiguity and to achieve qualitative understanding of the solutions without using equations. But before entering into the business we want to justify, at least partly, our setting, i.e., prior determination of all the remaining parameters besides δ and θ_{13}.

A. Problem of parameter degeneracy; set up of the problem

We assume that at the time that an experiment for measuring (δ, θ_{13}) is carried out all the remaining parameters in the MNS matrix, θ_{23}, $|\Delta m^2_{23}|$, θ_{12}, and Δm^2_{12}, are determined accurately. The discussion on how the experimental uncertainties affect the problem of parameter degeneracy is important, but is beyond the scope of this paper. It should be more or less true, because θ_{23} and Δm^2_{23} will be determined quite accurately by the future long-baseline experiments [24–26] up to the $\theta_{23} \leftrightarrow \frac{\pi}{2} - \theta_{23}$ ambiguity. Most notably, the expected sensitivities in the JHF-SK experiment in its phase I is [24]

$$\delta(\sin^2 2\theta_{23}) \simeq 10^{-2}$$
$$\delta(|\Delta m^2_{23}|) \simeq 4 \times 10^{-4}\mathrm{eV}^2 \quad (1)$$

at around $|\Delta m^2_{23}| = 3 \times 10^{-3}$ eV^2. On the other hand, the best place for accurate determination of θ_{12} and Δm^2_{12}, assuming the LMA MSW solar neutrino solution, is most probably the KamLAND experiment; the expected sensitivities are [27]

$$\delta(\tan^2 \theta_{12}) \simeq 10\%$$
$$\delta(\Delta m^2_{12}) \simeq 10\% \quad (2)$$

at around the LMA best fit parameters. Therefore, we feel that our setting, prior determination of all the mixing angles and Δm^2's besides δ, θ_{13} and the sign of Δm^2_{23} , is reasonable one at least in the first approximation.

B. Pictorial representation of parameter ambiguities

In this subsection we use CP and the T trajectory diagrams [10,12] to explain intuitively what is the problem of parameter degeneracy, and to achieve qualitative understanding of the solutions without using equations. In Fig. 1 we display four CP trajectories in the P-CP[P] bi-probability space which all have intersection at $P(\nu) = 1.9\%$ and CP[$P(\nu)$] = 2.6%. The four CP trajectories are drawn with four different values of θ_{13}, $\sin^2 2\theta_{13} = 0.055$, 0.050, 0.586, 0.472, and the former (latter) two trajectories correspond to positive (negative) Δm^2_{13}. The analytic expressions of the four degenerate solutions will be derived in Sec. IV. The neutrino energy E and the baseline length L are taken as $E = 250$ MeV and $L = 130$ km, respectively[1]. The setting anticipates an application to the CERN-Frejus project [28], where the regions with parameter ambiguities are widest. The values of all the remaining mixing parameters are given in the caption of Fig. 1.

---

[1] In all the figures of this paper we do not average over neutrino energy distributions as was performed in Refs. [10,12] but use a fixed neutrino energy specified for each figure.

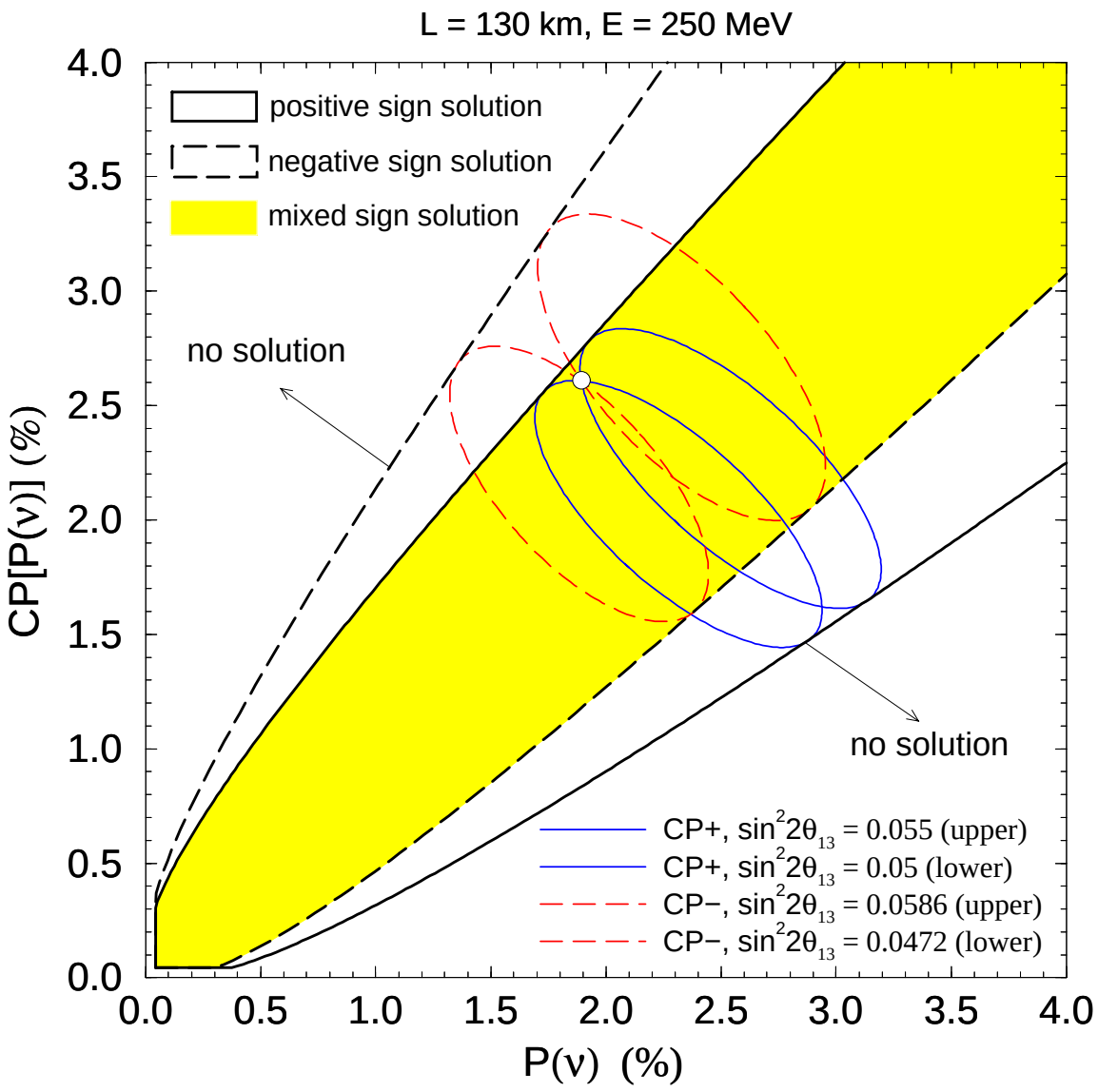

FIG. 1. An example of the degenerate solutions for the CERN-Frejius project in the $P(\nu) \equiv P(\nu_\mu \to \nu_e)$ verses $CP[P(\nu)] \equiv P(\bar{\nu}_\mu \to \bar{\nu}_e)$ plane. Between the solid (dashed) lines is the allowed region for positive (negative) Δm^2_{13} and the shaded region is where solution for both signs are allowed. The solid (dashed) ellipses are for positive (negative) Δm^2_{13} and they all meet at a single point. This is the CP parameter degeneracy problem. We have used a fixed neutrino energy of 250 MeV and a baseline of 130 km. The mixing parameters are fixed to be $|\Delta m^2_{13}| = 3 \times 10^{-3} eV^2$, $\sin^2 2\theta_{23} = 1.0$, $\Delta m^2_{12} = +5 \times 10^{-5} eV^2$, $\sin^2 2\theta_{12} = 0.8$ and $Y_e \rho = 1.5$ g cm^{-3}.

Figure 1 demonstrates that there is a four-hold degeneracy in the determination of (δ, θ_{13}) for a given set of $P(\nu)$ and CP$[P(\nu)]$. The region between the solid lines and the region between the dashed lines in Fig. 1 are the regions where two-fold degeneracies exist in the solutions of (δ, θ_{13}) for positive and negative Δm^2_{13} sectors, respectively. (See Eq. (48) in Sec. IV.) It is intuitively understandable that the region where degenerate solutions exists is the region swept over by the CP trajectories when the parameter θ_{13} is varied, while keeping other mixing parameters and the experimental conditions fixed. The shaded region is the region where the full four-hold degeneracy exists.

Now we turn to the T measurement. In Fig. 2 we display four T trajectories in the P-T$[P]$ bi-probability space which all have intersection at $P(\nu) = 1.7\%$ and T$[P(\nu)] = 2.5\%$. The four T trajectories are drawn with four different values of θ_{13}, $\sin^2 2\theta_{13} = 0.05$, 0.0427, 0.575, 0.490, and the former (latter) two trajectories correspond to positive (negative) Δm^2_{13}. Matter effects split the positive and negative Δm^2_{13} trajectories, see [12], thus different values of θ are required for mixed sign trajectories to overlap. The remaining mixing parameters and the experimental setting are the same as in Fig. 1.

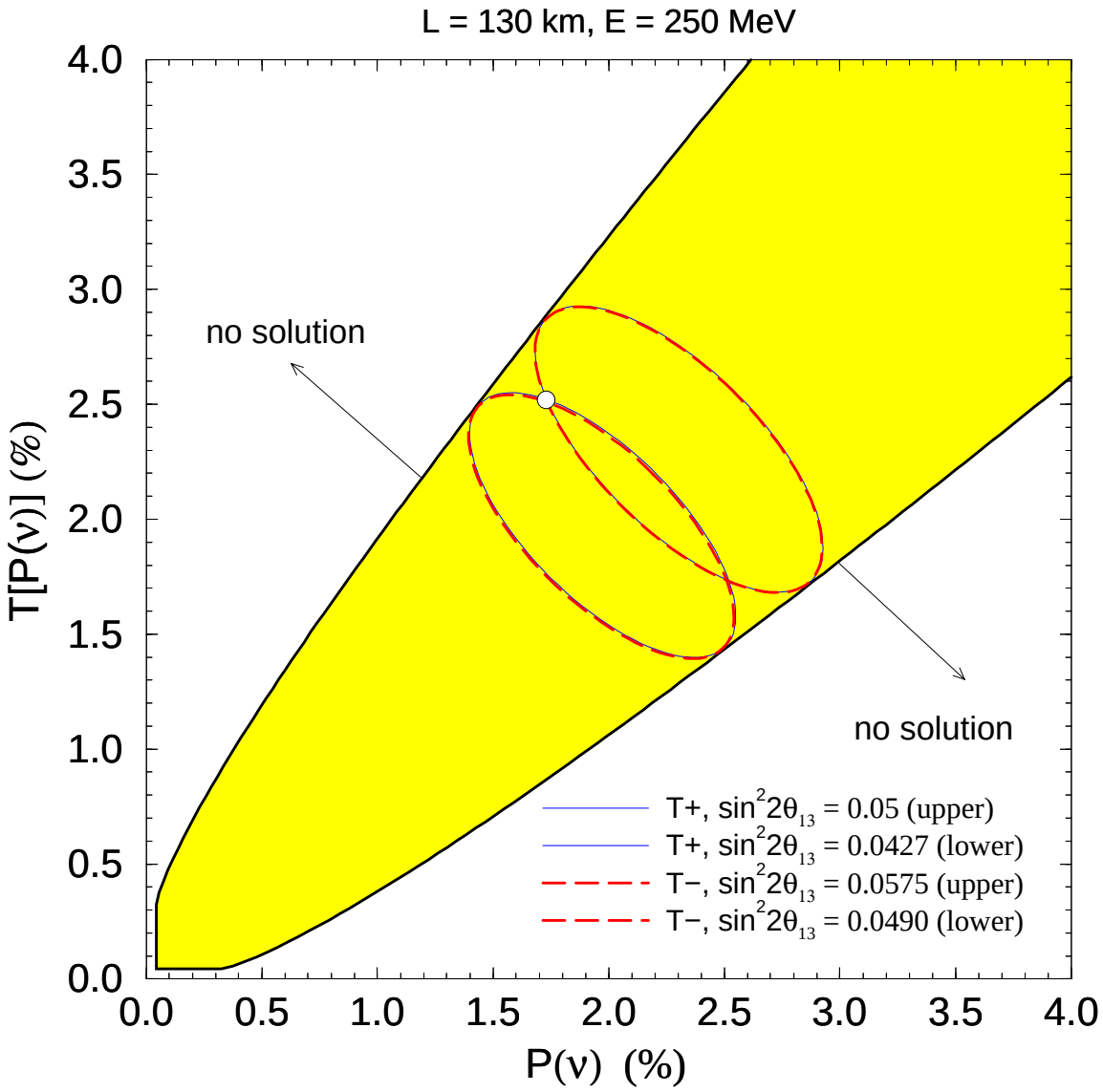

FIG. 2. An example of the degenerate solutions using the energy and path length of the CERN-Frejius project in the $P(\nu) \equiv P(\nu_\mu \to \nu_e)$ verses $T[P(\nu)] \equiv P(\nu_e \to \nu_\mu)$ plane. For this figure there is complete overlap in the region (shaded) that allows solutions for either sign of Δm^2_{13}. The solid (dashed) ellipses are for positive (negative) Δm^2_{13} and they all meet at the "measured point", (P, P^T) = (1.7, 2.5)%. This is the T-parameter degeneracy problem. Notice that for the each ellipse with positive Δm^2_{13} there is a completely degenerate ellipse with negative Δm^2_{13}. This feature will be explained in Sec. IIIc. Parameters are the same as in Fig. 1.

A clear and interesting difference from the CP diagram manifests itself already at this level, reflecting the highly symmetric nature of the T conjugate probabilities as will be made explicit in eq. (3). Namely, the two different-Δm^2_{13}-sign diagrams (the first and the third, and the second and fourth) completely overlap with each other. In the next section we will make it clear that the complete degeneracy originates from a symmetry. Therefore, discrimination of the sign of Δm^2_{13} is impossible in a single T-violation measurement experiment unless one of the solutions is excluded by an other experiment. We will demonstrate in Sec. III that the degeneracy is not accidental one specific to this particular case, but its existence is generic. There is always a four-hold degeneracy in T measurement.

III. PARAMETER DEGENERACY IN T-VIOLATION MEASUREMENTS

We start by presenting an analytic treatment of the problem of parameter degeneracy in T-violation measurements primarily because it is simpler and instructive. To do this we generalize the formalism developed by Burguet-Castell *et al.* [9] by treating the cases of positive and negative Δm^2_{13} simultaneously. It provides basis of our treatment of the degeneracy between the same as well as across the alternating Δm^2_{13}-sign probabilities. It will become clear from the following discussions that the treatment of the mixed-sign degenerate solutions, for both CP and T measurements, can be done as a straightforward generalization of the same-sign degeneracy case by simply taking account of duplication due to the alternating sign of Δm^2_{13} [10].

There are four basic equations satisfied by the T-conjugate probabilities in the case of T measurement for small $\sin\theta_{13}$:

$$\begin{aligned}
P(\nu)_+ &= X_+\theta^2 + Y_+\theta\cos\left(\delta + \frac{\Delta_{13}}{2}\right) + P_\odot \\
T[P(\nu)]_+ \equiv P^T(\nu)_+ &= X_+\theta^2 + Y_+\theta\cos\left(\delta - \frac{\Delta_{13}}{2}\right) + P_\odot \\
P(\nu)_- &= X_-\theta^2 + Y_-\theta\cos\left(\delta - \frac{\Delta_{13}}{2}\right) + P_\odot \\
T[P(\nu)]_- \equiv P^T(\nu)_- &= X_-\theta^2 + Y_-\theta\cos\left(\delta + \frac{\Delta_{13}}{2}\right) + P_\odot
\end{aligned} \tag{3}$$

where $X_\pm$ and $Y_\pm$ are given in Appendix, $P_\odot$ indicates the term which is related with solar neutrino oscillations, and $\Delta_{13} \equiv \frac{|\Delta m^2_{13}|L}{2E}$. Note that $\pm$ here refers to the sign of Δm^2_{13} and θ is an abbreviation of $\theta_{13} \simeq \sin\theta_{13}$. In the next subsections we discuss the possible solutions for θ and δ for a given measurement of both P and P^T for both positive and negative sign of Δm^2_{13}.

A. The same-sign degeneracy; T measurement

The treatment in this subsection applies for two overlapping T trajectories with the same sign of Δm^2_{13}. The degeneracy associated with alternating-sign trajectories will be explored in the next subsection.

There are two sets of approximate solutions of (3), θ_i and δ_i , where (i = 1,2) and (i = 3,4) denotes the solutions in the positive and negative Δm^2_{13} sectors, respectively. They are

$$\begin{aligned}
\theta_i &= \sqrt{\frac{P - P_\odot}{X_\pm}} - \frac{Y_\pm}{2X_\pm}\cos\left(\delta_i \pm \frac{\Delta_{13}}{2}\right) \\
\theta_i &= \sqrt{\frac{P^T - P_\odot}{X_\pm}} - \frac{Y_\pm}{2X_\pm}\cos\left(\delta_i \mp \frac{\Delta_{13}}{2}\right)
\end{aligned} \tag{4}$$

where $\pm$ correspond to solutions in positive and negative Δm^2_{13} sectors [2]. We then obtain, e.g., for the positive Δm^2_{13} sector

$$\begin{aligned}
\theta_2 - \theta_1 &= -\frac{Y_+}{2X_+}\left[(\cos\delta_2 - \cos\delta_1)\cos\left(\frac{\Delta_{13}}{2}\right) - (\sin\delta_2 - \sin\delta_1)\sin\left(\frac{\Delta_{13}}{2}\right)\right] \\
\theta_2 - \theta_1 &= -\frac{Y_+}{2X_+}\left[(\cos\delta_2 - \cos\delta_1)\cos\left(\frac{\Delta_{13}}{2}\right) + (\sin\delta_2 - \sin\delta_1)\sin\left(\frac{\Delta_{13}}{2}\right)\right]
\end{aligned} \tag{5}$$

which entails the degeneracy that if (θ_1, δ_1) is a solution so is

$$\theta_2 = \theta_1 + \frac{Y_+}{X_+}\cos\delta_1\cos\left(\frac{\Delta_{13}}{2}\right) \quad \text{and} \quad \delta_2 = \pi - \delta_1, \tag{6}$$

---

[2]The above solutions are exact solutions to the system of Eq. (3) if we were to add terms $Y^2_\pm\cos^2\left(\delta \pm \frac{\Delta_{13}}{2}\right)/(4X_\pm)$ to the equations, (3) . In what follows we have systematically ignored terms of $\mathcal{O}(Y^2_\pm/X_\pm)$.

in addition to the trivial solution. A similar degeneracy holds also for the negative Δm^2_{13} sector, that is, if (θ_3, δ_3) is a solution so is

$$\theta_4 = \theta_3 + \frac{Y_-}{X_-}\cos\delta_3 \cos\left(\frac{\Delta_{13}}{2}\right) \quad \text{and} \quad \delta_4 = \pi - \delta_3. \tag{7}$$

Both of these same sign Δm^2_{13} degeneracies are in matter though they look like the vacuum degeneracies as discussed in [10]. Notice that if the experimental setup is chosen such that $\cos\left(\frac{\Delta_{13}}{2}\right) = 0$ [8] or nature has chosen $\cos\delta = 0$ then the same sign degeneracies are removed.

B. The mixed-sign degeneracy; T measurement

Let us now examine the problem of parameter degeneracy which involves positive and negative Δm^2_{13}. The basic equations (3) can be approximately solved for mixed sign situation as:

$$\begin{aligned}
\theta_1 &= \sqrt{\frac{P - P_\odot}{X_+}} - \frac{Y_+}{2X_+}\cos\left(\delta_1 + \frac{\Delta_{13}}{2}\right) \\
\theta_1 &= \sqrt{\frac{P^T - P_\odot}{X_+}} - \frac{Y_+}{2X_+}\cos\left(\delta_1 - \frac{\Delta_{13}}{2}\right) \qquad (8) \\
\theta_3 &= \sqrt{\frac{P - P_\odot}{X_-}} - \frac{Y_-}{2X_-}\cos\left(\delta_3 - \frac{\Delta_{13}}{2}\right) \\
\theta_3 &= \sqrt{\frac{P^T - P_\odot}{X_-}} - \frac{Y_-}{2X_-}\cos\left(\delta_3 + \frac{\Delta_{13}}{2}\right). \qquad (9)
\end{aligned}$$

We will now exactly determine θ and δ using the above set of approximate solutions, (8) and (9), as our starting point. First,

$$\sin\delta_1 \sin\frac{\Delta_{13}}{2} = -\frac{\sqrt{X_+}}{Y_+}\left(\sqrt{P - P_\odot} - \sqrt{P^T - P_\odot}\right) \tag{10}$$

$$\sin\delta_3 \sin\frac{\Delta_{13}}{2} = \frac{\sqrt{X_-}}{Y_-}\left(\sqrt{P - P_\odot} - \sqrt{P^T - P_\odot}\right) \tag{11}$$

and $\cos\delta_i$ is given by $\cos\delta_i = \pm\sqrt{1 - \sin^2\delta_i}$. Using these $\cos\delta_i$ the values of θ are given by

$$\theta_1 = \frac{\left(\sqrt{P - P_\odot} + \sqrt{P^T - P_\odot}\right)}{2\sqrt{X_+}} - \frac{Y_+}{2X_+}\cos\delta_1 \cos\frac{\Delta_{13}}{2} \tag{12}$$

$$\theta_3 = \frac{\left(\sqrt{P - P_\odot} + \sqrt{P^T - P_\odot}\right)}{2\sqrt{X_-}} - \frac{Y_-}{2X_-}\cos\delta_3 \cos\frac{\Delta_{13}}{2}. \tag{13}$$

To relate these alternating sign solutions we use the identity, see Appendix,

$$\frac{\sqrt{X_+}}{Y_+} = -\frac{\sqrt{X_-}}{Y_-} \tag{14}$$

derivable under the Cervera *et al.* approximation[3]. Then, it follows that

$$\begin{aligned} \sin\delta_1 &= \sin\delta_3 \\ (\cos\delta_1 + \cos\delta_3)\cos\frac{\Delta_{13}}{2} &= -2\frac{\sqrt{X_+}}{Y_+}\left(\sqrt{X_+}\theta_1 - \sqrt{X_-}\theta_3\right) \end{aligned} \tag{15}$$

One can choose without loss of generality $\delta_3 = \pi - \delta_1$ as a solution of (15). Then, for a given P and P^T measurement, apart from (θ_1, δ_1) there are three other solutions[4] given by

$$\begin{aligned} \theta_2 &= \theta_1 + \frac{Y_+}{X_+}\cos\delta_1\cos\left(\frac{\Delta_{13}}{2}\right) \quad \text{and} \quad \delta_2 = \pi - \delta_1 \\ \theta_3 &= \sqrt{\frac{X_+}{X_-}}\theta_1 \qquad\qquad\qquad\quad \text{and} \quad \delta_3 = \pi - \delta_1 \\ \theta_4 &= \theta_3 - \frac{Y_-}{X_-}\cos\delta_1\cos\left(\frac{\Delta_{13}}{2}\right) \quad \text{and} \quad \delta_4 = \delta_1 \end{aligned} \tag{16}$$

Therefore, there is no ambiguity in determination of δ in T violation measurement apart from the one $\delta \to \pi - \delta$ independent of the sign of Δm^2_{13}. Fortunately, this degeneracy does not obscure existence or non-existence of leptonic T (or CP) violation. This feature arises because of highly constrained nature of system (3) of T-conjugate probabilities.

The physically allowed region of the T diagram is determined by the constraint that $\sin^2\delta_i \leq 1$ which in terms of P and P^T is

$$\left(\sqrt{P - P_\odot} - \sqrt{P^T - P_\odot}\right)^2 \quad \leq \quad \frac{Y_+^2}{X_+}\sin^2\left(\frac{\Delta_{13}}{2}\right) = \frac{Y_-^2}{X_-}\sin^2\left(\frac{\Delta_{13}}{2}\right) \tag{17}$$

---

[3] Unless Eq. (14) holds we get into trouble because then Eqs. (8) or (9) does not allow the (same-sign) solution $\theta_1 = \theta_2$ and $\delta_1 = \delta_2$, which must exist as shown in Ref. [12]. Therefore, use of the formula of oscillation probability obtained by Cervera *et al.* who summed up all order matter effect is essential.

[4] As a convention, we have chosen $\cos\delta_1 \leq 0$ so that for $\Delta_{13} \leq \pi$, $\theta_1 \geq \theta_2$ and $\theta_3 \geq \theta_4$.

and is the same region for both signs of Δm^2_{13} because of the identity Eq.(14). In Fig. 2, this region is the shaded region using the CERN-Frejius parameters. At the boundary of the allowed physical region $\cos\delta = 0$ and the same sign degeneracy vanishes, however, the opposite sign degeneracy is non-zero.

We define the fractional differences, $\Delta\theta/\bar{\theta}$, by

$$\left(\frac{\Delta\theta}{\bar{\theta}}\right)_{ij} \equiv \frac{\theta_i - \theta_j}{(\theta_i + \theta_j)/2}, \tag{18}$$

to quantify how different the two degenerate solutions are. In fact, one can obtain simple expressions for the various fractional differences;

$$\left(\frac{\Delta\theta}{\bar{\theta}}\right)_{12} = \left(\frac{\Delta\theta}{\bar{\theta}}\right)_{34} = \frac{-2Y_+ \cos\delta_1 \cos\left(\frac{\Delta_{13}}{2}\right)}{\sqrt{X_+}\left(\sqrt{P - P_\odot} + \sqrt{P^T - P_\odot}\right)}, \tag{19}$$

$$\left(\frac{\Delta\theta}{\bar{\theta}}\right)_{31} = \left(\frac{\Delta\theta}{\bar{\theta}}\right)_{42} = 2\frac{(\sqrt{X_+} - \sqrt{X_-})}{(\sqrt{X_+} + \sqrt{X_-})}, \tag{20}$$

$$\left(\frac{\Delta\theta}{\bar{\theta}}\right)_{14} \approx \frac{-2Y_+ \cos\delta_1 \cos\left(\frac{\Delta_{13}}{2}\right)}{\sqrt{X_+}\left(\sqrt{P - P_\odot} + \sqrt{P^T - P_\odot}\right)} - 2\left(\frac{\sqrt{X_+} - \sqrt{X_-}}{\sqrt{X_+} + \sqrt{X_-}}\right), \tag{21}$$

$$\left(\frac{\Delta\theta}{\bar{\theta}}\right)_{32} \approx \frac{-2Y_+ \cos\delta_1 \cos\left(\frac{\Delta_{13}}{2}\right)}{\sqrt{X_+}\left(\sqrt{P - P_\odot} + \sqrt{P^T - P_\odot}\right)} + 2\left(\frac{\sqrt{X_+} - \sqrt{X_-}}{\sqrt{X_+} + \sqrt{X_-}}\right). \tag{22}$$

The same sign fractional difference, (1,2) and (3,4), decreases with increasing P and P^T and thus θ, whereas the first mixed sign fractional difference, (3,1) and (4,2), is independent of the size of P and P^T and thus θ. The second and third mixed sign fractional differences, (1,4) and (2,3), are similar to the same sign fractional difference but off set by an energy dependent constant. The relationship between the fractional difference in the measured quantity $\sin^2 2\theta$ and θ is simply

$$\frac{\sin^2 2\theta_i - \sin^2 2\theta_j}{(\sin^2 2\theta_i + \sin^2 2\theta_j)/2} \approx 2\frac{\theta_i - \theta_j}{(\theta_i + \theta_j)/2} = 2\left(\frac{\Delta\theta}{\bar{\theta}}\right)_{ij}. \tag{23}$$

for $1 \gg \theta_i, \theta_j \gg |\theta_i - \theta_j|$.

In Fig. 3 thru 5 we have plotted the differences in the allowed θ solutions divided by half the sum for the CERN-Frejus, JHF-SK and FNAL-NuMI [29] possible experiments

using $\nu_\mu \to \nu_e$ and its T-conjugate $\nu_e \to \nu_\mu$. The regions where this fractional difference is small are regions where the parameter degeneracy inherent in such measurements is only important once the experimental resolution on θ for a fixed solution is of the same size or smaller. Notice that near the boundaries on the allowed region the fractional differences are small for the same sign solutions. For the mixed sign, either the (1,4) or (3,2) fractional difference plots have a line for which the fractional difference is zero. This line can be understood as follows; for a given small value of θ the positive and negative Δm^2_{13} ellipses overlap and intersect at two points. As θ varies these intersection points give us this line with zero mixed sign fractional difference.

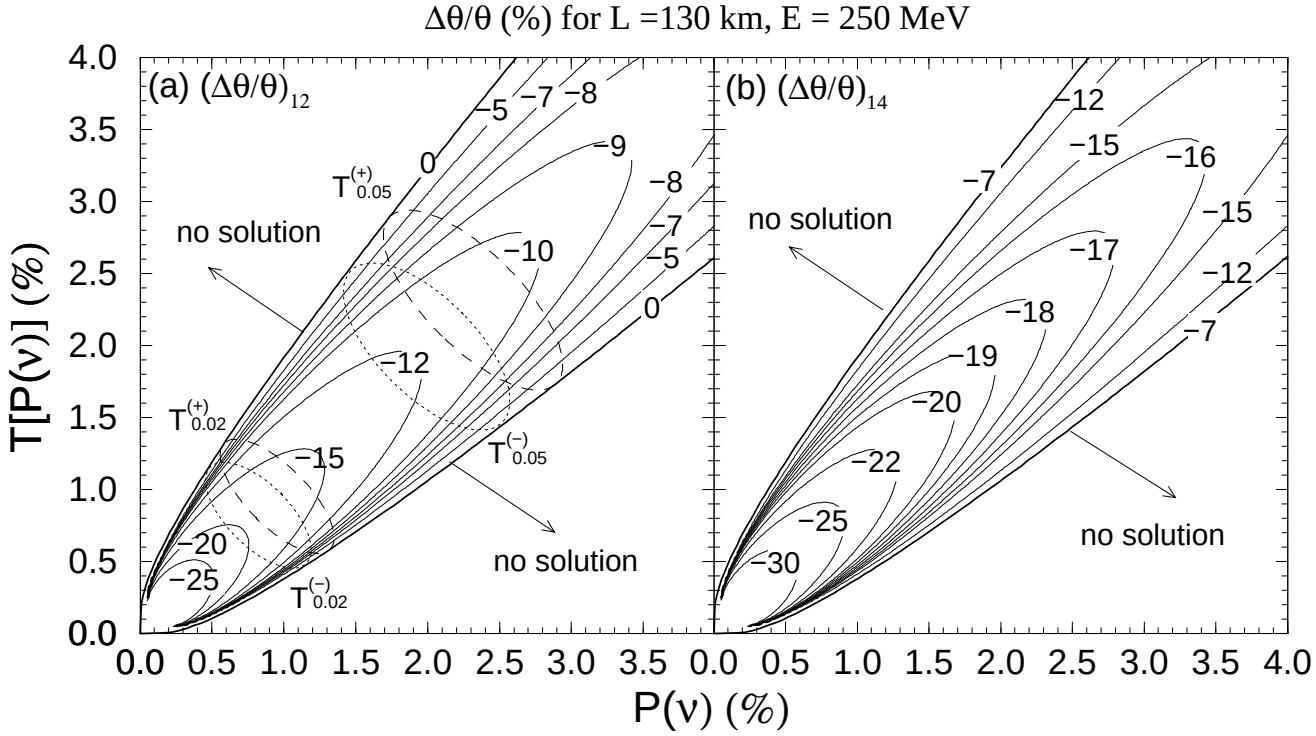

FIG. 3. The iso-fractional differences, as a %, for the allowed solutions for the mixing angle θ_{13} in the $P(\nu) \equiv P(\nu_\mu \to \nu_e)$ verses $T[P(\nu)] \equiv P(\nu_e \to \nu_\mu)$ plane for the CERN-Frejius project. The fractional differences for solutions (3,4) is identical to that for (1,2) and the fractional difference for (3,2) equals the fractional difference for (1,4) plus or minus a constant, see eq. (19)-(22). In this case the fractional difference (3,2) has a zero contour. The parameters are the same as in Fig. 1. The ellipses are labelled $T^{(\pm)}_{\sin^2 2\theta_{13}}$ to show the relevant size of $\sin^2 2\theta_{13}$ for this figure.

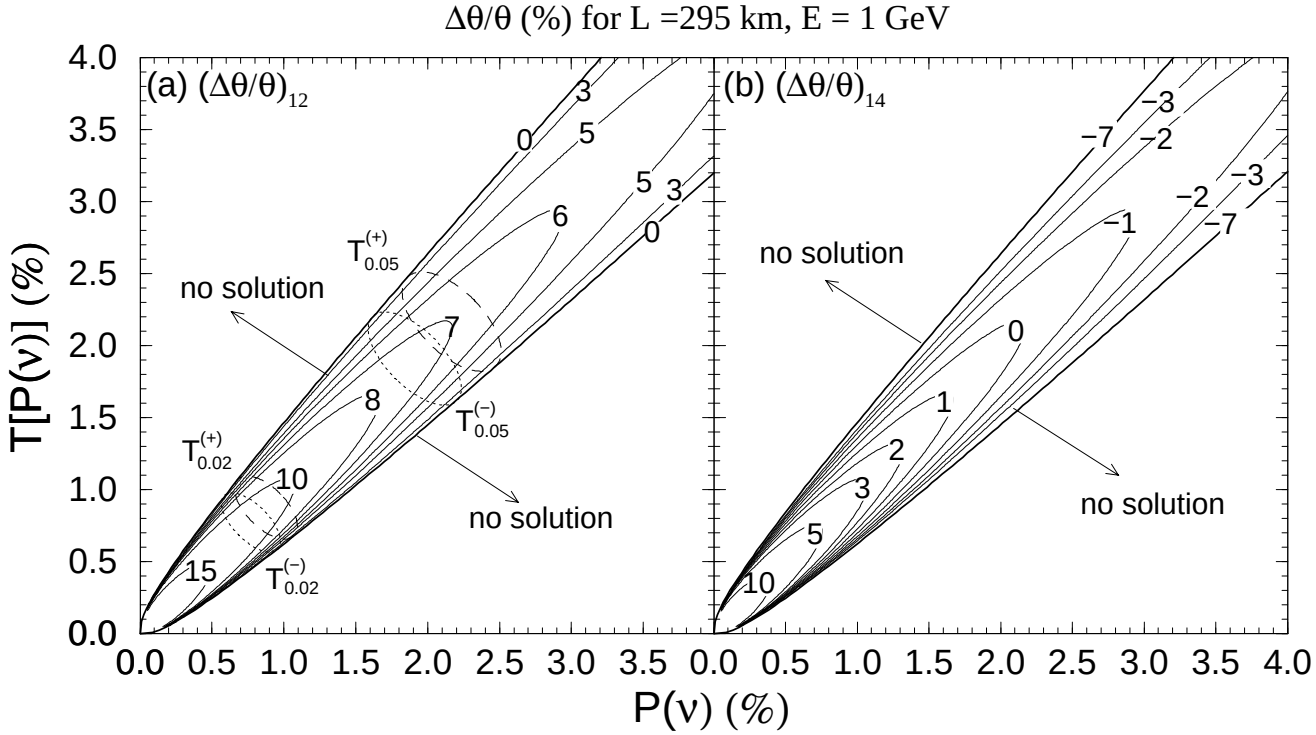

FIG. 4. The iso-fractional differences, as a %, for the allowed solutions for the mixing angle θ_{13} in the $P(\nu) \equiv P(\nu_\mu \to \nu_e)$ verses $T[P(\nu)] \equiv P(\nu_e \to \nu_\mu)$ plane for the JHK-SK project. The fractional differences for solutions (3,4) is identical to that for (1,2) and the fractional difference for (3,2) equals the fractional difference for (1,4) plus or minus a constant, see eq. (19)-(22). The zero contour appearing in the (1,4) fractional difference is explained in the text. The parameters are the same as in Fig. 1. The ellipses are labelled as in Fig.3.

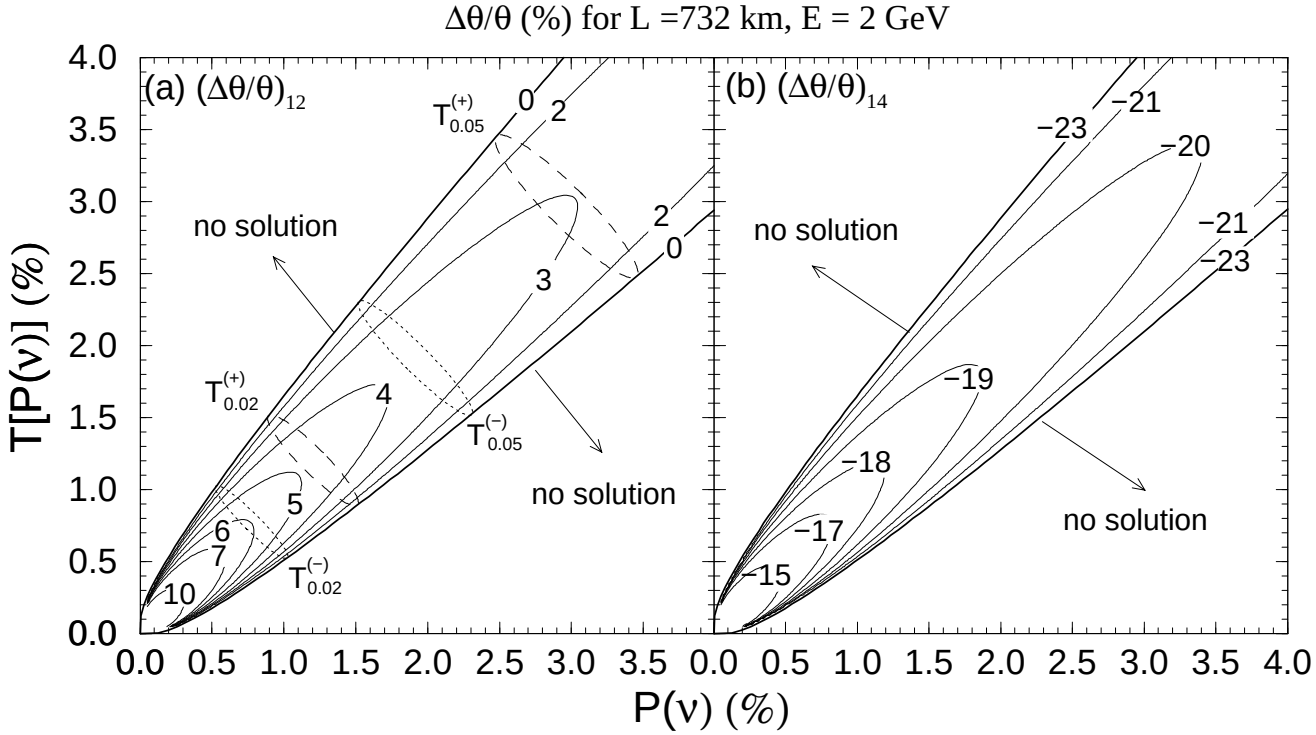

FIG. 5. The iso-fractional differences, as a %, for the allowed solutions for the mixing angle θ_{13} in the $P(\nu) \equiv P(\nu_\mu \to \nu_e)$ verses $T[P(\nu)] \equiv P(\nu_e \to \nu_\mu)$ plane for the FNAL-NUMI project. The fractional differences for solutions (3,4) is identical to that for (1,2) and the fractional difference for (3,2) equals the fractional difference for (1,4) plus or minus a constant, see eq. (19)-(22). At very small probability the (1,4) fractional difference has a zero contour. The parameters are the same as in Fig. 1. The ellipses are labelled as in Fig.3.

C. Symmetry between the two alternating-Δm^2_{13}-sign T diagrams

The observant reader will notice that there is in a general one-to-one correspondence between the solutions with positive Δm^2_{13}, labelled 1 and 2, and those solutions with negative Δm^2_{13}, labelled 3 and 4, in Eq. (16) by using the identity, Eq. (14). In fact this correspondence applies not only to the solutions but to the complete T diagram. For a given T trajectory with positive Δm^2_{13} there always exists a T trajectory with negative Δm^2_{13} with a different value of θ, which nevertheless completely overlaps the positive trajectory, see Fig. 2. This surprising phenomenon occurs because there exists a symmetry in T probability system

defined in Eq. (3).

One can observe from eq. (3) that a positive Δm^2_{13} trajectory which is defined by the first two equations of (3) can be used to generate a negative Δm^2_{13} trajectory which completely overlaps with the original one by the transformation

$$\begin{aligned} \delta &\to \pi - \delta \\ \theta &\to \sqrt{\frac{X_-}{X_+}}\theta \end{aligned} \tag{24}$$

This means that for a measure set of P and P^T there is always two set of solutions with different sign of Δm^2_{13}. There is no way to resolve this ambiguity because the two T trajectories are completely degenerate. It should be noticed that this situation occurs no matter how large a matter effect at much longer baseline. In such a case, two T trajectories with the same θ_{13} but opposite sign of Δm^2_{13} are far apart, and one would have expected that there is no ambiguity in determination of the sign of Δm^2_{13}. Hence, there is a "no-go theorem" for the determination of the sign of Δm^2_{13} by a single T violation measurement. The possible cases in which the "theorem" is circumvented are, as mentioned in Introduction, (a) one of the solutions is excluded, for example, by the CHOOZ constraint, or (b) some additional information, such as energy distribution of the appearance electrons or another T-violation measurement with different parameters, is added.

IV. PARAMETER DEGENERACY IN CP-VIOLATION MEASUREMENTS

We now turn to the analytic treatment of the parameter degeneracy in CP-violation measurements. We proceed in an analogous way to the analytic treatment of T-violation given in sec. III.

We start with the four basic CP equations for small $\sin\theta_{13}$:

$$\begin{aligned} P(\nu)_+ &= X_+\theta^2 + Y_+\theta\cos\left(\delta + \frac{\Delta_{13}}{2}\right) + P_\odot \\ \mathrm{CP}[P(\nu)]_+ \equiv \bar{P}(\nu)_+ &= \bar{X}_+\theta^2 + \bar{Y}_+\theta\cos\left(\delta - \frac{\Delta_{13}}{2}\right) + P_\odot \end{aligned}$$

$$P(\nu)_- = X_-\theta^2 + Y_-\theta\cos\left(\delta - \frac{\Delta_{13}}{2}\right) + P_\odot$$
$$\mathrm{CP}[P(\nu)]_- \equiv \bar{P}(\nu)_- = \bar{X}_-\theta^2 + \bar{Y}_-\theta\cos\left(\delta + \frac{\Delta_{13}}{2}\right) + P_\odot \tag{25}$$

where $X_\pm$ and $Y_\pm$ are given in Appendix. As before, $P_\odot$ indicates the term which is related with solar neutrino oscillations, $\Delta_{13} \equiv \frac{|\Delta m^2_{13}|L}{2E}$, the $\pm$ here refers to the sign of Δm^2_{13} and θ is an abbreviation of $\theta_{13} \simeq s_{13}$.

Note that there exist relations among coefficients;

$$X_\pm \equiv X(\pm\Delta m^2_{13}, a) \tag{26}$$
$$\bar{X}_\pm = X(\pm\Delta m^2_{13}, -a) \tag{27}$$

In leading order in $\frac{\Delta m^2_{12}}{\Delta m^2_{13}}$, there exist further relations,

$$X_+ = \bar{X}_- \quad \text{and} \quad X_- = \bar{X}_+ \tag{28}$$

which follows from the CP-CP relation [12] (see Appendix). Finally, it follows under the approximation of Cervera *et al.* [21] that

$$Y_+ = -\bar{Y}_-, \quad Y_- = -\bar{Y}_+. \tag{29}$$

We fully utilize the symmetry relationships (28) and (29) in the unified treatment of the same-sign and the mixed-sign degeneracies. The basic equations (25) can be solved for generic mixed sign situation as:

$$\theta_1 = \sqrt{\frac{P - P_\odot}{X_+}} - \frac{Y_+}{2X_+}\cos\left(\delta_1 + \frac{\Delta_{13}}{2}\right) \tag{30}$$
$$\theta_1 = \sqrt{\frac{\bar{P} - P_\odot}{X_-}} + \frac{Y_-}{2X_-}\cos\left(\delta_1 - \frac{\Delta_{13}}{2}\right) \tag{31}$$
$$\theta_3 = \sqrt{\frac{P - P_\odot}{X_-}} - \frac{Y_-}{2X_-}\cos\left(\delta_3 - \frac{\Delta_{13}}{2}\right) \tag{32}$$
$$\theta_3 = \sqrt{\frac{\bar{P} - P_\odot}{X_+}} + \frac{Y_+}{2X_+}\cos\left(\delta_3 + \frac{\Delta_{13}}{2}\right) \tag{33}$$

The solution of these equations are:

$$\sin\delta_{1,2}= \frac{1}{D}\left[-C^{(+)}\sin\frac{\Delta_{13}}{2}\Delta P_{+} \pm C^{(-)}\cos\frac{\Delta_{13}}{2}\sqrt{D-(\Delta P_{+})^2}\right] \tag{34}$$

$$\sin\delta_{3,4}= \frac{1}{D}\left[-C^{(+)}\sin\frac{\Delta_{13}}{2}\Delta P_{-} \mp C^{(-)}\cos\frac{\Delta_{13}}{2}\sqrt{D-(\Delta P_{-})^2}\right] \tag{35}$$

$$\theta_{1,2} = \frac{1}{2D^{(-)}}\left[\frac{\sqrt{(P-P_{\odot})X_{+}}}{Y_{+}}+\frac{\sqrt{(\bar{P}-P_{\odot})X_{-}}}{Y_{-}}+\sin\delta_{1,2}\sin\frac{\Delta_{13}}{2}\right] \tag{36}$$

$$\theta_{3,4} = \frac{1}{2D^{(-)}}\left[\frac{\sqrt{(P-P_{\odot})X_{-}}}{Y_{-}}+\frac{\sqrt{(\bar{P}-P_{\odot})X_{+}}}{Y_{+}}-\sin\delta_{3,4}\sin\frac{\Delta_{13}}{2}\right] \tag{37}$$

where

$$D \equiv C^{(+)^2}\sin^2\left(\frac{\Delta_{13}}{2}\right)+C^{(-)^2}\cos^2\left(\frac{\Delta_{13}}{2}\right) \tag{38}$$

$$C^{(\pm)} \equiv \frac{1}{2}\left(\frac{Y_{+}}{X_{+}}\mp\frac{Y_{-}}{X_{-}}\right) \tag{39}$$

$$D^{(\pm)} \equiv \frac{1}{2}\left(\frac{X_{+}}{Y_{+}}\mp\frac{X_{-}}{Y_{-}}\right) \tag{40}$$

$$\Delta P_{\pm} \equiv \sqrt{\frac{P-P_{\odot}}{X_{\pm}}}-\sqrt{\frac{\bar{P}-P_{\odot}}{X_{\mp}}} \tag{41}$$

The sign in (35) is determined relative to (34) so that it reproduces the pair of degenerate solutions in the case of a precisely determined value of θ_{13} [12]. It should be noticed that provided $\sqrt{D-(\Delta P_{\pm})^2}$ is real the constraint $|\sin\delta_i| \leq 1$ is satisfied automatically in (34) and (35).

Let us focus first on the features of the same-sign degenerate solution. The set (θ_i, δ_i) with $i = 1, 2$ ($i = 3, 4$) describes two degenerate solutions with positive (negative) Δm^2_{13} for given values of P and $\bar{P}$. Of course, they reproduce the relationships obtained by Burguet-Castell *et al* in [9]:

$$\sin\delta_2 - \sin\delta_1 = -2\left(\frac{\sin\delta_1+z\cos\delta_1}{1+z^2}\right) \tag{42}$$

$$\theta_2-\theta_1= \left(\frac{\sin\delta_1+z\cos\delta_1}{1+z^2}\right)\left(\frac{C^{(+)^2}-C^{(-)^2}}{C^{(-)}}\right)\sin\left(\frac{\Delta_{13}}{2}\right) \tag{43}$$

where

$$z = \frac{C^{(+)}}{C^{(-)}}\tan\left(\frac{\Delta_{13}}{2}\right) \tag{44}$$

Let us illuminate how the relative phases between δ's between these degenerate solutions can be obtained in a transparent way. Toward the goal we first calculate $\cos\delta_i$. $\cos\delta_{1,2}$ and $\cos\delta_{3,4}$ can be obtained from (34) and (35), respectively, by replacing of $C^{(\pm)}$ by $\mp C^{(\mp)}$ and $\sin\frac{\Delta_{13}}{2}$ by $\cos\frac{\Delta_{13}}{2}$ and vice versa. One can show by using these results that

$$\cos(\delta_1+\delta_2)=\cos(\delta_3+\delta_4)=\frac{1-z^2}{1+z^2}, \tag{45}$$

which implies that

$$\begin{aligned}\delta_2&=\pi-\delta_1+\arccos((z^2-1)/(z^2+1))\\ \delta_4&=\pi-\delta_3+\arccos((z^2-1)/(z^2+1)).\end{aligned} \tag{46}$$

Thus in the allowed region of bi-probability space δ_2 (δ_4) differs from $\pi-\delta_1$ ($\pi-\delta_3$) by a constant, $\arccos((z^2-1)/(z^2+1))$, which depends on the energy and path length of the neutrino beam but not on the mixing angle θ. Near the oscillation maximum, $z\to\infty$, this constant vanishes so that $\delta_2\simeq\pi-\delta_1$ and $\delta_3\simeq\pi-\delta_4$ as noticed in [9].

For the mixed-sign degenerate solution one can show that

$$\begin{aligned}\cos(\delta_1-\delta_3)&=\frac{\left(\Delta P_+\Delta P_- -\sqrt{D-\Delta P_+^2}\sqrt{D-\Delta P_-^2}\right)}{D}\\ \sin(\delta_1-\delta_3)&=\frac{\left(\Delta P_+\sqrt{D-\Delta P_-^2}+\Delta P_-\sqrt{D-\Delta P_+^2}\right)}{D}\end{aligned} \tag{47}$$

One can show, for example, $\cos(\delta_1-\delta_3)=-1$ and $\sin(\delta_1-\delta_3)=0$ in the $\bar{P}\to P$ limit by noting that $\Delta P_-=-\Delta P_+$ in the limit. It means that $\delta_3=\delta_1+\pi$ (mod. 2π), in agreement with the result obtained in Ref. [12].

The conditions for existence of the same-sign solution are

$$D-(\Delta P_+)^2\geq 0 \quad \text{and} \quad D-(\Delta P_-)^2\geq 0 \tag{48}$$

for positive and negative Δm^2_{13}, respectively. The condition for existence of the mixed-sign solution is the intersection of the two regions which satisfy the conditions of eq. (48). An example of the regions satisfying conditions for existence of the same-sign as well as mixed-sign solutions are depicted in Fig. 1.

The maximum value of P and $\bar{P}$ which allows mixed sign solutions is determined by $D-(\Delta P_+)^2 = D-(\Delta P_-)^2 = 0$ with $P=\bar{P}$. This occurs for a critical value of P given by

$$P_{crit} = P_\odot + \frac{X_+ X_- D}{(\sqrt{X_+}-\sqrt{X_-})^2} \tag{49}$$

which can be used to determine the critical value of θ as

$$\theta_{crit} = \frac{C^{(+)} \sin^2 \frac{\Delta_{13}}{2}}{2D^{(-)}\sqrt{D}}. \tag{50}$$

There is no degeneracy in the value of θ at this critical point, *i.e.* $\theta_1 = \theta_2 = \theta_3 = \theta_4$. An example of this can be seen in Fig. 8. At the first peak in the oscillation probability, $\Delta_{13} = \pi$, the value of the critical θ is simply given by

$$\theta_{crit}(\Delta_{13}=\pi) = \frac{|Y_+|}{\sqrt{X_+}(\sqrt{X_+}-\sqrt{X_-})}. \tag{51}$$

As $\Delta_{13} \to 2\pi$, the critical θ goes to zero and so does the oscillation probabilities P and $\bar{P}$ as this is the position of the first trough in the oscillation probabilities.

In Fig. 6 thru 8 we have plotted the fractional difference, $\left(\frac{\Delta\theta}{\theta}\right)$, see eq. (18), for the CERN-Frejius, JHF-SK and FNAL-NUMI possible experiments using $\nu_\mu \to \nu_e$ and its CP-conjugate $\bar{\nu}_\mu \to \bar{\nu}_e$. The regions where this fractional difference is small are regions where the parameter degeneracy inherent in such measurements is only important once the experimental resolution on θ for a fixed solution is of the same size or smaller. Notice that near the boundaries on the allowed region the fractional differences are small for the same sign solutions. For the mixed sign, (1,3), fractional difference plots there is a zero along the diagonal. This is explained by the fact that in our approximation the positive and negative Δm^2_{13} ellipses, for a given θ, intersect along the diagonal. Fig. 9 thru 11 are similar to Fig. 6 thru 8 expect that the size of solar Δm^2_{12} has been increased by a factor of two to $1\times 10^{-4}\text{eV}^2$. Notice that the parameter degeneracies problem is more pronounced as the solar Δm^2 is increased. At even larger values of Δm^2_{12}, our approximations become less reliable.

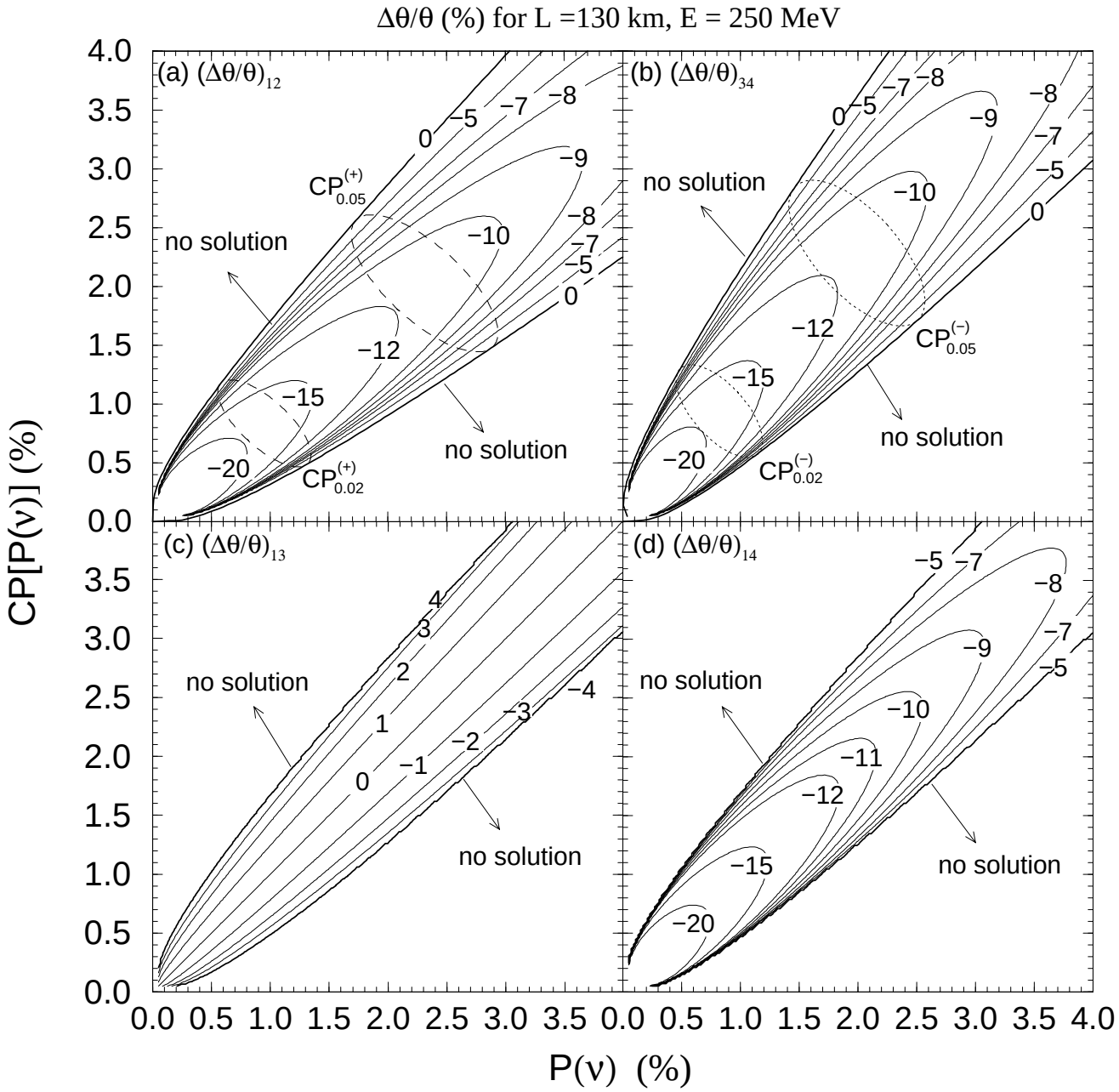

FIG. 6. The iso-fractional differences, as a %, for the allowed solutions for the mixing angle θ_{13} in the $P(\nu) \equiv P(\nu_\mu \to \nu_e)$ verses $CP[P(\nu)] \equiv P(\bar{\nu}_\mu \to \bar{\nu}_e)$ plane for the CERN-Frejius project. The parameters are the same as in Fig. 1 with $\Delta m^2_{12} = 5 \times 10^{-5}$ eV^2. The dashed ellipses are labelled $CP^{(\pm)}_{\sin^2 2\theta_{13}}$ to show the relevant size of $\sin^2 2\theta_{13}$ for this figure.

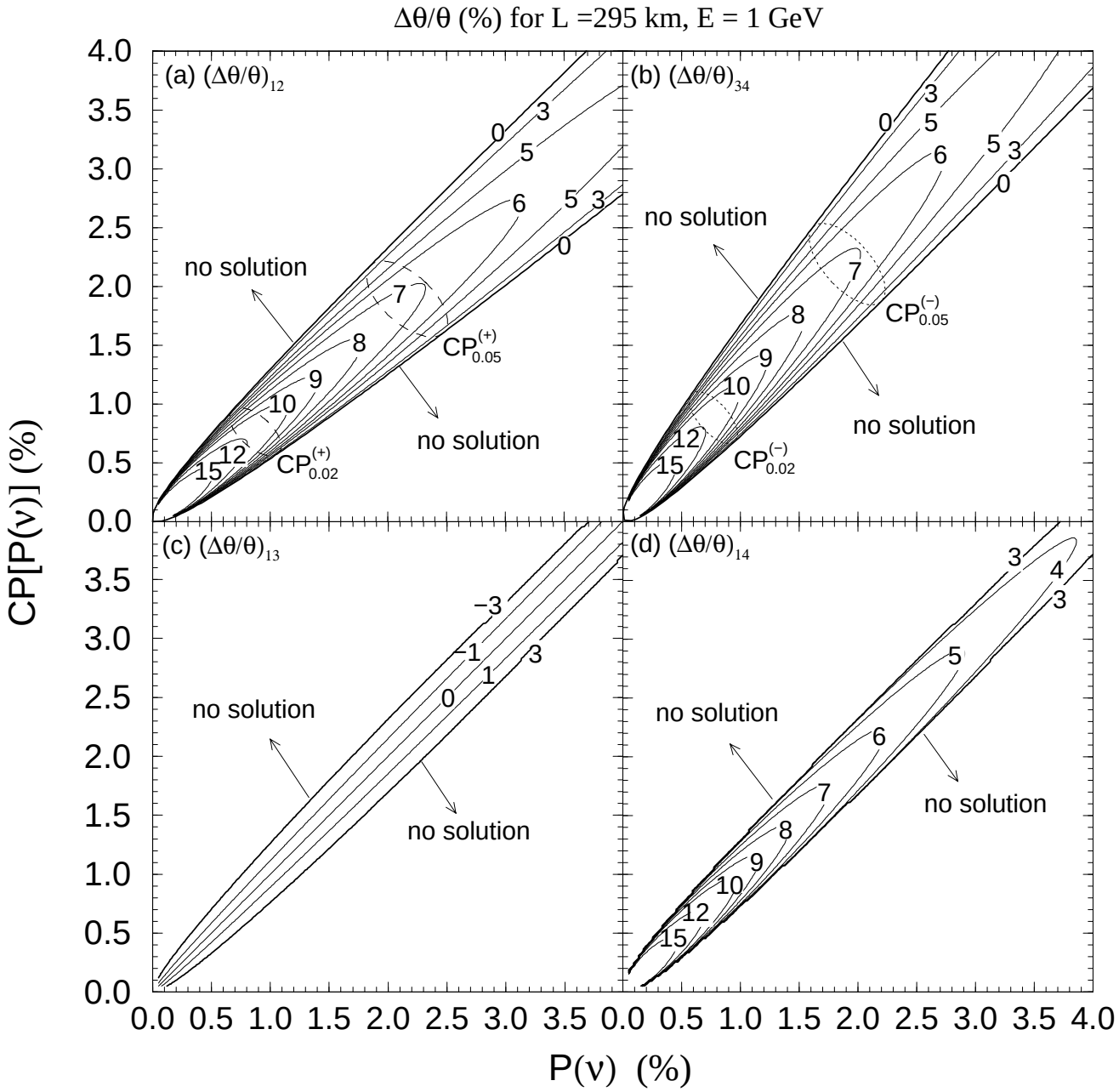

FIG. 7. The iso-fractional differences, as a %, for the allowed solutions for the mixing angle θ_{13} in the $P(\nu) \equiv P(\nu_\mu \to \nu_e)$ verses $CP[P(\nu)] \equiv P(\bar{\nu}_\mu \to \bar{\nu}_e)$ plane for the JHF-SK project. The parameters are the same as in Fig. 1 with $\Delta m^2_{12} = 5 \times 10^{-5}$ eV^2. The ellipses are labelled as in Fig.6.

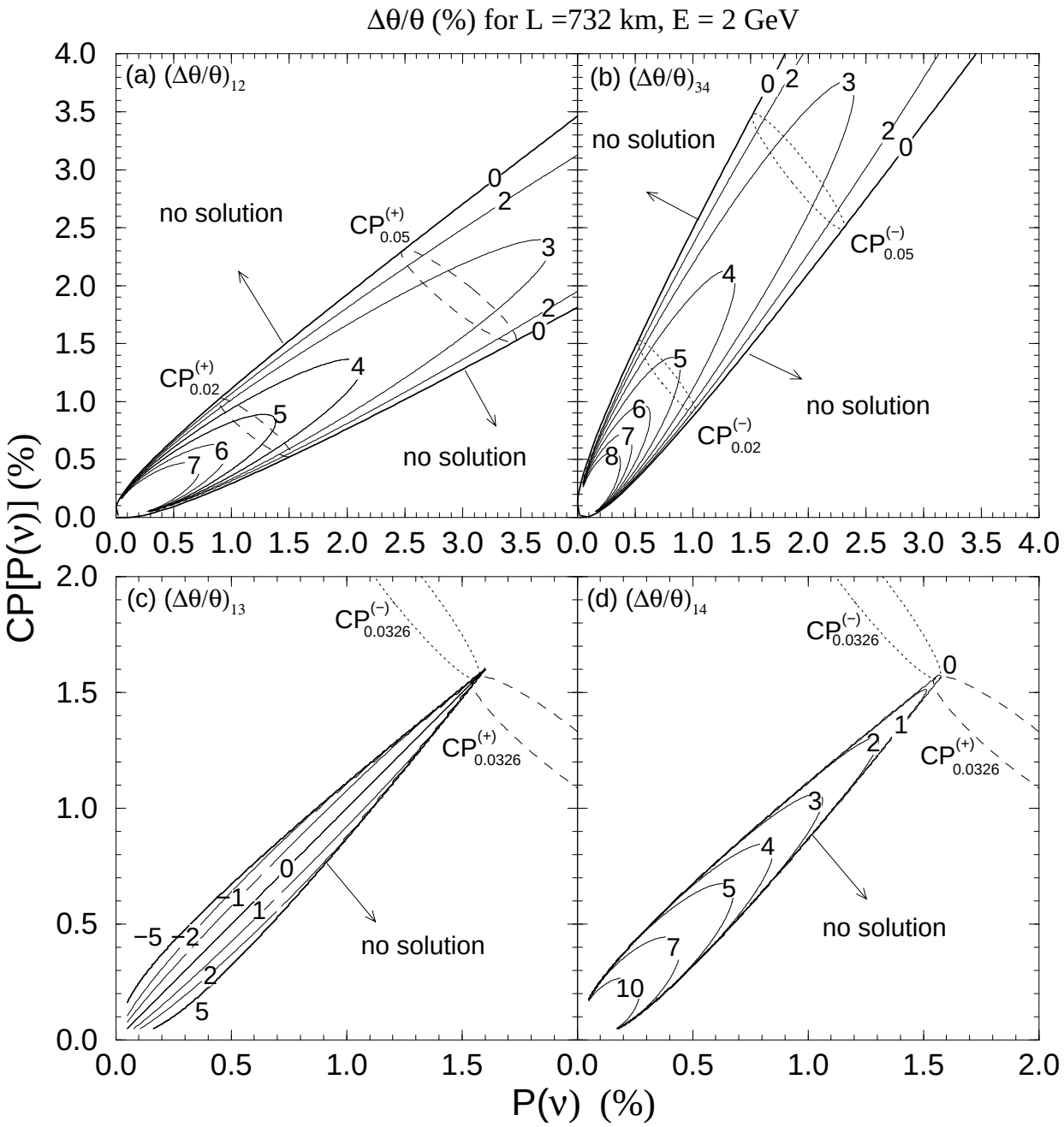

FIG. 8. The iso-fractional differences, as a %, for the allowed solutions for the mixing angle θ_{13} in the $P(\nu) \equiv P(\nu_\mu \to \nu_e)$ verses $CP[P(\nu)] \equiv P(\bar{\nu}_\mu \to \bar{\nu}_e)$ plane for the FNAL-NUMI project. The mixed sign fractional differences, $(\Delta\theta/\bar{\theta})_{13 \text{ and } 14}$ terminate at around $P = CP[P] \approx 1.6\%$ because above this probability the sign of Δm^2_{13} is determined, as discussed in the text. The critical value of P ($\approx 1.6\%$) and $\sin^2 2\theta_{13}$ (≈ 0.033) can be calculated from eq. (49) and (50). The parameters are the same as in Fig. 1 with $\Delta m^2_{12} = 5 \times 10^{-5}$ eV^2. The ellipses are labelled as in Fig.6.

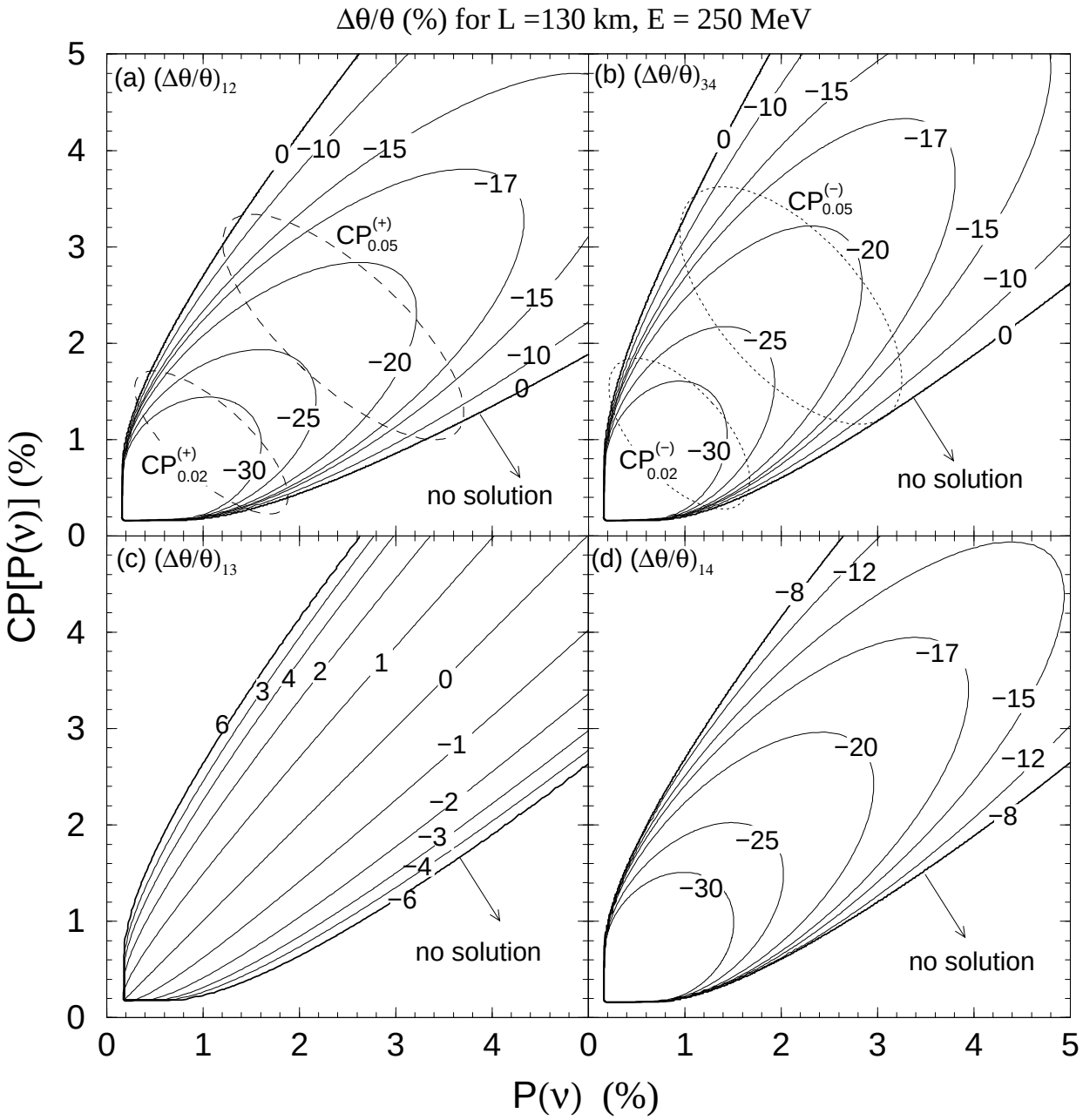

FIG. 9. The iso-fractional differences, as a %, for the allowed solutions for the mixing angle θ_{13} in the $P(\nu) \equiv P(\nu_\mu \to \nu_e)$ verses $CP[P(\nu)] \equiv P(\bar{\nu}_\mu \to \bar{\nu}_e)$ plane for the CERN-Frejius project. The parameters are the same as in Fig. 1 except for the solar Δm^2_{12} which is set to $1 \times 10^{-4} eV^2$ for this plot. The ellipses are labelled as in Fig.6.

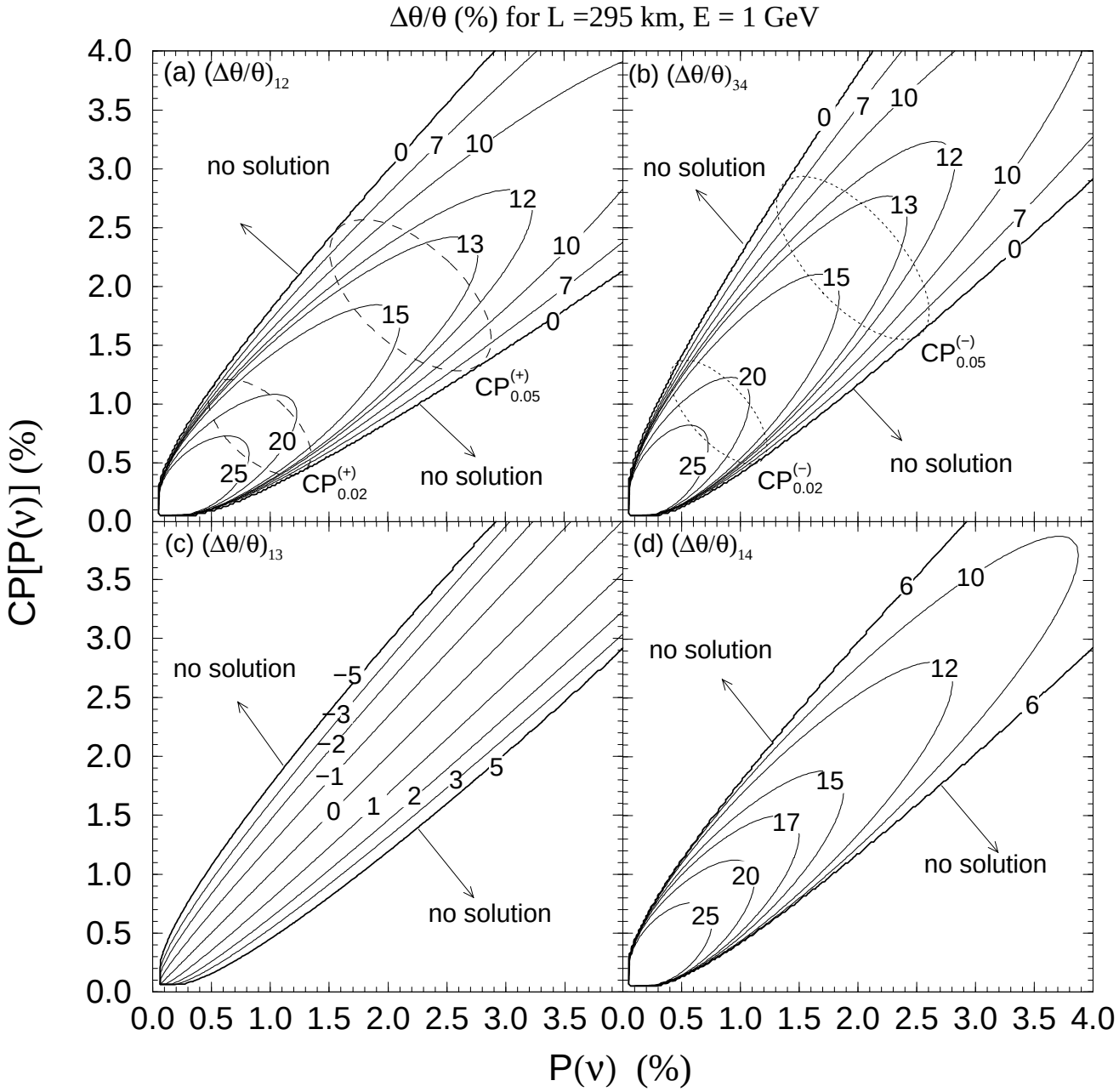

FIG. 10. The iso-fractional differences, as a %, for the allowed solutions for the mixing angle θ_{13} in the $P(\nu) \equiv P(\nu_\mu \to \nu_e)$ verses $CP[P(\nu)] \equiv P(\bar{\nu}_\mu \to \bar{\nu}_e)$ plane for the JHF-SK project. The parameters are the same as in Fig. 1 except for the solar Δm^2_{12} which is set to $1 \times 10^{-4} eV^2$ for this plot. The ellipses are labelled as in Fig.6.

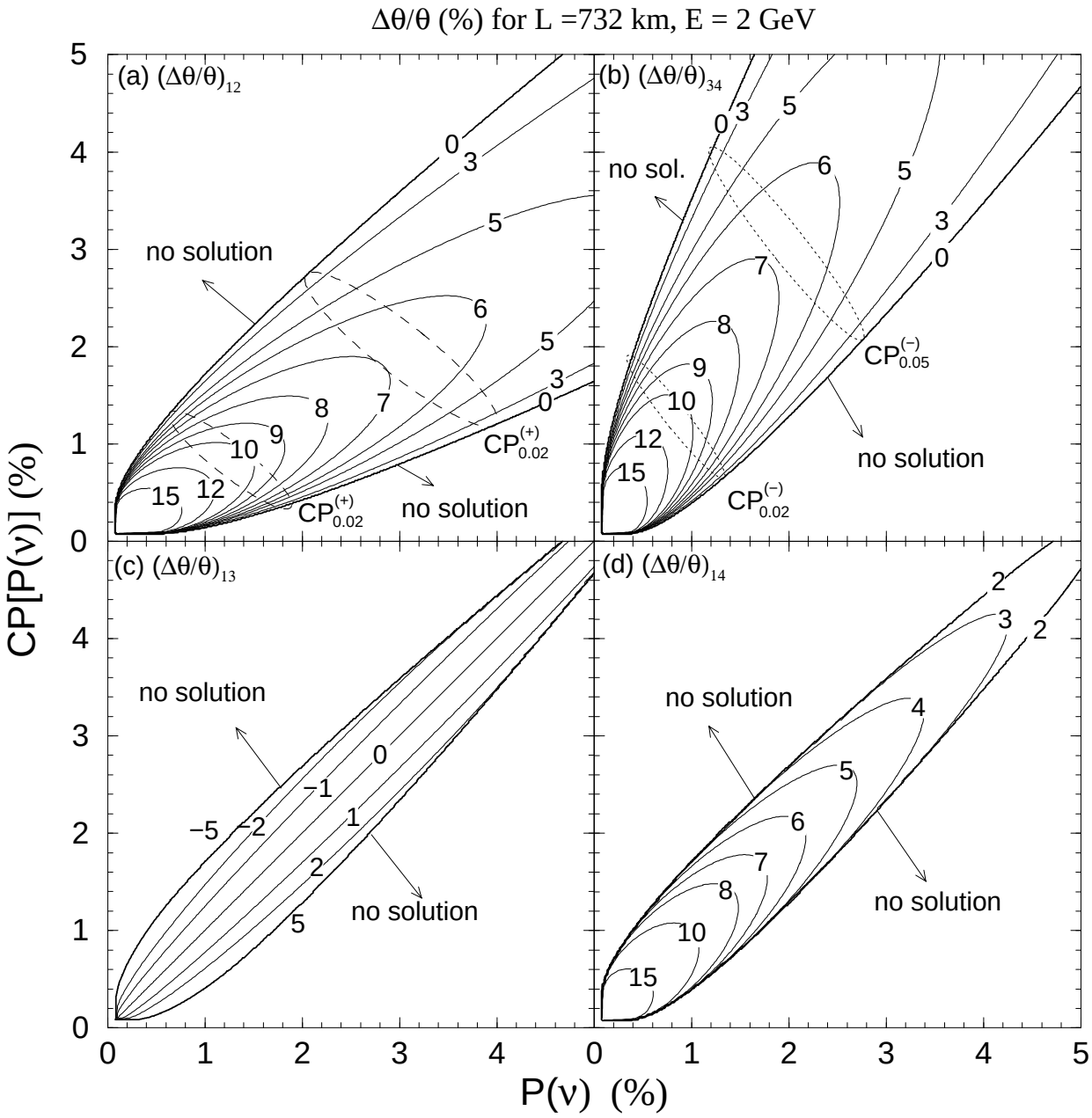

FIG. 11. The iso-fractional differences, as a %, for the allowed solutions for the mixing angle θ_{13} in the $P(\nu) \equiv P(\nu_\mu \to \nu_e)$ verses $CP[P(\nu)] \equiv P(\bar{\nu}_\mu \to \bar{\nu}_e)$ plane for the FNAL-NUMI project. The parameters are the same as in Fig. 1 except for the solar Δm^2_{12} which is set to $1 \times 10^{-4} eV^2$ for this plot. The ellipses are labelled as in Fig.6.

V. SUMMARY AND CONCLUSION

In this paper we have given a complete analytic treatment of the parameter degeneracy issue for θ_{13}, sign of Δm^2_{13} and the CP and T violating phase δ that appears in neutrino

oscillations. For a given neutrino flavor transition probability and its CP or T conjugate probability we have derived the allowed values of θ_{13}, sign of Δm^2_{13} and the CP and T violating phase δ. We have given explicit expressions of degenerate solutions and obtained, among other things, exact formulas for the relationship between solutions of δ's up to the correction of order $\left(\frac{\Delta m^2_{12}}{\Delta m^2_{13}}\right)^2$.

In general there is a four-fold degeneracy, two allowed values of θ_{13} for both signs of Δm^2_{13}. This is always true for the T violation measurement whereas for the CP violation measurement the four-fold degeneracy can be reduced to two-fold degeneracy if matter effects are sufficiently large, or we live close to the region $\delta \sim \pi/2$ or $3\pi/2$. The significance of matter effects dependence on the energy of the neutrino beam, the separation between the source and the detector as well as the density of matter between them. The fractional difference of θ_{13} between the various solutions has been calculated which can be compared with the experimental sensitivity for a given setup to determine whether or not the degeneracy issue is significant or not.

For the possible future experimental setups CERN-Frejius, JHK-SK and FNAL-NUMI we have given numerical results for the channel $\nu_\mu \to \nu_e$ and its CP and T conjugate. The CP conjugate being most relevant for these future Super-beam experiments. For the CERN-Frejius, JHF-SK and FNAL-NUMI experimental setups the parameter degeneracy issue is only relevant once the experimental resolution on the determination of θ_{13} is better than 15%, 10% and 5% respectively, assuming a transition probability near 1% and a $\Delta m^2_{12} = 5 \times 10^{-5} eV^2$, see Fig. 6 - 8. At larger values of Δm^2_{12} the parameter degeneracy issue becomes more important. These iso-fractional difference plots are useful for comparing the sensitivity of different experimental setups, neutrino energy, path length and experimental sensitivity, to this parameter degeneracy issue.

ACKNOWLEDGMENTS

HM thanks Theoretical Physics Department of Fermilab for warm hospitality extended to him through the summer visitors program in 2002. This work was supported by the Grant-in-Aid for Scientific Research in Priority Areas No. 12047222, Japan Ministry of Education, Culture, Sports, Science, and Technology. Fermilab is operated by URA under DOE contract No. DE-AC02-76CH03000.

VI. APPENDIX

The standard flavor transition probability for neutrino oscillations in the $\nu_\mu \to \nu_e$ channel can be written as

$$P(\nu)_\pm = X_\pm \theta^2 + Y_\pm \theta \cos\left(\delta \pm \frac{\Delta_{13}}{2}\right) + P_\odot \tag{52}$$

where the $\pm$ signs in $X_\pm$ and $Y_\pm$ refer to positive or negative values of Δm^2_{13}, θ is an abbreviation for $\sin\theta_{13}$ and $P_\odot$ indicates the terms related to solar neutrino oscillations. For details on the approximations used in deriving this transition probability see ref. [21]. All other channels used in this paper, $\nu_e \to \nu_\mu$ and $\bar{\nu}_\mu \to \bar{\nu}_e$, can also be expressed with the same variables, see Sec. III and IV.

The coefficients $X_\pm$ and $Y_\pm$ are determined by

$$X_\pm = 4 s^2_{23} \left(\frac{\Delta_{13}}{B_\mp}\right)^2 \sin^2\left(\frac{B_\mp}{2}\right), \tag{53}$$

$$Y_\pm = \pm 8 c_{12} s_{12} c_{23} s_{23} \left(\frac{\Delta_{12}}{aL}\right)\left(\frac{\Delta_{13}}{B_\mp}\right) \sin\left(\frac{aL}{2}\right) \sin\left(\frac{B_\mp}{2}\right) \tag{54}$$

$$P_\odot = c^2_{23} \sin^2 2\theta_{12} \left(\frac{\Delta_{12}}{aL}\right)^2 \sin^2\left(\frac{aL}{2}\right) \tag{55}$$

with

$$\Delta_{ij} \equiv \frac{|\Delta m^2_{ij}| L}{2E} \quad \text{and} \quad B_\pm \equiv |aL \pm \Delta_{13}|, \tag{56}$$

where $a = \sqrt{2} G_F N_e$ denotes the index of refraction in matter with G_F being the Fermi constant and N_e a constant electron number density in the earth.

Obviously from the above definitions, $X_\pm$ and $Y_\pm$ satisfy the identity

$$\frac{Y_+}{\sqrt{X_+}} = -\frac{Y_-}{\sqrt{X_-}} \tag{57}$$

which is used throughout this paper.

REFERENCES

[1] Kamiokande Collaboration, Y. Fukuda *et al.*, Phys. Lett. **B335** (1994) 237;
Super-Kamiokande Collaboration, Y. Fukuda *et al.*, Phys. Rev. Lett. **81** (1998) 1562; *ibid.* **85** (2000) 3999.

[2] Homestake Collaboration, K. Lande *et al.*, Astrophys. J. **496** (1998) 505;
SAGE Collaboration, J. N. Abdurashitov *et al.*, Phys. Rev. C **60** (1999) 055801;
GALLEX Collaboration, W. Hampel *et al.*, Phys. Lett. B **447** (1999) 127;
Super-Kamiokande Collaboration, S. Fukuda *et al.*, Phys. Rev. Lett. **86** (2001) 5651; *ibid.* **86** (2001) 5656;
SNO Collaboration, Q. R. Ahmad *et al.*, Phys. Rev. Lett. **87** (2001) 071301; *ibid.* **89** (2002) 011301; **89** (2002) 011302.

[3] K2K Collaboration, S. H. Ahn *et al.*, Phys. Lett. B **511** (2001) 178;
K. Nishikawa, Talk presented at XXth International Conference on Neutrino Physics and Astrophysics (Neutrino 2002), May 25-30, 2002, Munich, Germany.

[4] Z. Maki, M. Nakagawa and S. Sakata, Prog. Theor. Phys. **28** (1962) 870.

[5] M. B. Smy, hep-ex/0202020; SNO Collaboration, Q. R. Ahmad *et al.*, **89** (2002) 011302; J. N. Bahcall, M. C. Gonzalez-Garcia, and C. Peña-Garay, hep-ph/0204314; V. Barger et al., Phys. Lett. B **537** (2002) 179; A. Bandyopadhyay *et al.*, hep-ph/0204286;
P.C. de Holanda, A.Yu. Smirnov hep-ph/0205241; G. L. Fogli *et al.*, hep-ph/0206162; M. Maltoni *et al.*, hep-ph/0207227.

[6] S. P. Mikheev and A. Y. Smirnov, Nuovo Cim. C **9** (1986) 17;
L. Wolfenstein, Phys. Rev. D **17** (1978) 2369.

[7] CHOOZ Collaboration, M. Apollonio *et al.*, Phys. Lett. B **420** (1998) 397;
ibid. B **466** (1999) 415; See also, The Palo Verde Collaboration, F. Boehm *et al.*, Phys. Rev. D **62** (2000) 072002.

[8] T. Kajita, H. Minakata, and H. Nunokawa, Phys. Lett. **B528** (2002) 245 [hep-ph/0112345].

[9] J. Burguet-Castell, M.B. Gavela, J.J. Gomez-Cadenas, P. Hernandez and O. Mena, Nucl. Phys. B **608** (2001) 301.

[10] H. Minakata and H. Nunokawa, JHEP **0110** (2001) 001 [hep-ph/0108085].

[11] V. Barger, D. Marfatia, and K. Whisnant, Phys. Rev. D **65** (2002) 073023.

[12] H. Minakata, H. Nunokawa, and S. J. Parke, Phys. Lett B, **B537** (2002) 249 [hep-ph/0204171].

[13] J. Arafune and J. Sato, Phys. Rev. **D55** (1997) 1653; J. Arafune, M. Koike and J. Sato, Phys. Rev. **D56** (1997) 3093 [Erratum *ibid.* **D 60** (1999) 119905];
H. Minakata and H. Nunokawa, Phys. Rev. **D57** (1998) 4403; Phys. Lett. **B413** (1997) 369; *ibid.* **B495** (2000) 369;
K. Dick, M. Freund, M. Lindner and A. Romanino, Nucl. Phys. B **562** (1999) 29;
O. Yasuda, Acta. Phys. Polon. **B 30** (1999) 3089; M. Koike and J. Sato, Phys. Rev. **D61** (2000) 073012; Erratum *ibid.* **D 62** (2000) 079903.

[14] S. J. Parke and T. J. Weiler, Phys. Lett. **B501** (2001) 106.

[15] H. Minakata and H. Nunokawa, Nucl. Phys. Proc. Suppl. **110** (2002) 404 [hep-ph/0111131].

[16] V. Barger, D. Marfatia, and K. Whisnant, hep-ph/0206038.

[17] P. Huber, M. Lindner, and W. Winter, hep-ph/0204352.

[18] A. Donini, D. Meloni, and P. Migliozzi, hep-ph/0206034.

[19] J. Burguet-Castell, M.B. Gavela, J.J. Gomez-Cadenas, P. Hernandez and O. Mena, hep-ph/0207080.

[20] K. Kimura, A. Takamura and H. Yokomakura, Phys. Lett. **B537** (2002) 86; hep-ph/0205295.

[21] A. Cervera, A. Donini, M. B. Gavela, J. J. Gomez Cadenas, P. Hernandez, O. Mena and S. Rigolin, Nucl. Phys. **B579** (2000) 17 [*Erratum-ibid.* **B593** (2000) 731].

[22] The idea of low-energy conventional "superbeam" for measuring leptonic CP violation may be traced back to
H. Minakata and H. Nunokawa, Phys. Lett. **B495** (2000) 369; Nucl. Instrum. Meth. **A472** (2001) 421; J. Sato, Nucl. Instrum. Meth. **A472** (2001) 434; B. Richter, hep-ph/0008222.

[23] C. Albright *et al.*, hep-ex/0008064; V. Barger, S. Geer, R. Raja and K. Whisnant, Phys. Rev. D **63** (2001) 113011; J. Pinney and O. Yasuda, Phys. Rev. D **64** (2001) 093008.

[24] Y. Itow *et al.*, *The JHF-Kamioka neutrino project*, hep-ex/0106019.

[25] The MINOS Collaboration, P. Adamson *et al.*, *MINOS Detectors Technical Design Report, Version 1.0*, NuMI-L-337, October 1998.

[26] OPERA Collaboration, M. Guler *et al.*, *OPERA: An Appearance Experiment to Search for Nu/Mu $\longleftrightarrow$ Nu/Tau Oscillations in the CNGS Beam. Experimental Proposal*, CERN-SPSC-2000-028, CERN-SPSC-P-318, LNGS-P25-00, Jul 2000.

[27] H. Murayama and A. Pierce, Phys. Rev. **D65** (2002) 013012.
See also, A. de Gouvêa and C. Peña-Garay, Phys. Rev. **D64** (2001) 113011; V. Barger, D. Marfatia, and B. P. Wood, Phys. Lett. **B498** (2001) 53; R. Barbieri and A. Strumia, JHEP **0012** (2000) 016.

[28] J. J. Gomez-Cadenas *et al.* (CERN working group on Super Beams Collaboration), hep-ph/0105297.

[29] http://www-off-axis.fnal.gov/loi/loi.ps